



ELSEVIER

Available online at www.sciencedirect.com

SCIENCE @ DIRECT®

Physics Letters A 309 (2003) 15–23

PHYSICS LETTERS A

www.elsevier.com/locate/pla

A folded Fabry–Perot cavity for optical sensing in gravitational wave detectors

F. Marin^{a,*}, L. Conti^b, M. De Rosa^c

^a *INFN, Sezione di Firenze, and Dipartimento di Fisica, Università di Firenze, and LENS, Via Sansone 1, I-50019 Sesto Fiorentino, Firenze, Italy*

^b *INFN, Sezione di Padova, and Dipartimento di Fisica, Università di Padova, Via Marzolo 8, I-35131 Padova, Italy*

^c *INFN, Sezione di Firenze, and INOA, Largo Fermi 6, I-50125 Firenze, Italy*

Received 9 January 2003; received in revised form 9 January 2003; accepted 28 January 2003

Communicated by P.R. Holland

Abstract

The sensitivity of standard optical schemes for the readout of weak vibrations is limited thermal and radiation pressure fluctuations induced by the small interrogation area. We propose and analyze an optical configuration allowing to overcome this problem and optimize the sensitivity of the new generation of massive gravitational wave detectors.

© 2003 Elsevier Science B.V. All rights reserved.

PACS: 04.80.Nn; 42.79.-e

Keywords: Fabry–Perot cavity; Gravitational wave detectors; Thermal noise; Radiation pressure

1. Introduction

The research devoted to the realization of detectors for gravitational waves (gw) has seen substantial progress since the first experiments in the early 60s. However, it is now commonly accepted that, to open the possibility of a gw astronomy, a further substantial advance in sensitivity is necessary. To reach this goal a new generation of gw detectors is being studied. This activity concerns both long baseline interferometers (an example is LIGO2 [1]) and massive detectors, for which the most advanced designs are based on hollow spheres equipped with large mass resonant transducers [2] and wideband ‘dual’ detectors. The last configuration can be implemented with two nested spheres [3], an inner solid one and a hollow outer one, or two cylinders [4], and the signal is directly read from the gap between the two nested masses.

While long interferometers naturally employ long Fabry–Perot cavities (FP) in the two arms, also for resonant detectors the use of optical techniques for the displacement detection was considered in the past [5] and a complete

* Corresponding author.

E-mail address: marin@lens.unifi.it (F. Marin).

optical readout system has recently been operated on a room-temperature Weber bar [6]. Interferometric techniques can compete with the standard capacitive and inductive sensors which are used in cryogenic bars and they are excellent candidates for the necessary further extension of the sensitivity.

Optimizing the displacement sensitivity of a FP interferometer requires an increase of the input laser power and/or of the cavity finesse, up to the quantum limit given by the balance between the shot-noise effects in the detection and the back-action exerted by radiation pressure. A really quantum-limited detection can only be obtained if thermal noise is negligible.

The optical readout considered in Ref. [3] for the dual-sphere detector is based on a FP cavity with a finesse of 10^6 and laser power of about 1 W (in a conservative design) or 7 W (to reach the quantum limit at the design frequency of 1.3 kHz). The shot-noise limited displacement sensitivity corresponds respectively to $7 \times 10^{-45} \text{ m}^2/\text{Hz}$ and $10^{-45} \text{ m}^2/\text{Hz}$.¹ Thermal noise is negligible respectively for $Q/T > 2 \times 10^7 \text{ K}^{-1}$ and $Q/T > 2 \times 10^8 \text{ K}^{-1}$, where Q is the mechanical quality factor and T the temperature of the massive resonator. This calculation only considers the global detector response for evaluating both thermal noise and radiation pressure effects, using a normal mode expansion. On the other hand, one should also take into account local effects, due to surface deformation, for both thermal noise [7–10] and radiation pressure [11].

The rigorous analysis of local thermal noise sources is the subject of several recent works. The internal thermal noise of the test masses was studied by Levin [7] and by Liu and Thorne [8], who showed an important dependence on the size of the region which is interrogated. Besides these thermal fluctuations, called Brownian noise, two further noise sources must be considered, as pointed out by Braginsky et al. [9] and calculated on a wide frequency range by Cerdonio et al. [10]: a first one is due to fluctuations in the temperature (thermodynamic noise); a second one is due to the heating of the mirrors caused by the laser power in the cavity (photothermal noise). Both effects give rise to displacement fluctuations through the thermal expansion coefficient. As discussed in Ref. [10], around 1 K the material to be used in the mirror substrates is probably sapphire. In that case, thermal fluctuations are dominated by Brownian noise. The same work also reports the calculation of the ‘local’ radiation pressure effect.

Both effects can be calculated from the susceptibility $\chi(\omega)$ describing the mechanical response of the mirror to an exerted pressure [7,10]. From the fluctuation–dissipation theorem we obtain the spectral power of the Brownian noise

$$S_{\text{Br}}(\omega) = \frac{4k_{\text{B}}T}{\omega} \text{Im}[\chi(\omega)], \quad (1)$$

where k_{B} is the Boltzmann constant. The displacement noise due to radiation pressure fluctuations is given by

$$S_{\text{rp}}(\omega) = |\chi(\omega)|^2 \left(\frac{2}{c}\right)^2 S_{\text{cav}}, \quad (2)$$

where c is the speed of the light and S_{cav} is the noise spectral power of the radiation impinging on the mirror. If the mirror is part of a FP cavity of finesse F and a shot-noise limited laser with power P_{in} and optical frequency ν is resonant with the cavity, we have

$$S_{\text{cav}} = 2h\nu \left(\frac{F}{\pi}\right)^2 P_{\text{in}}. \quad (3)$$

If we consider a single Gaussian spot on a half-infinite mirror, for the low-frequency susceptibility we can use [12]

$$|\chi^{\text{single}}| = \frac{1}{\pi^{1/2}w} \frac{1 - \sigma^2}{Y}, \quad (4)$$

$$\text{Im}[\chi(\omega)] \simeq \phi |\chi(\omega)|, \quad (5)$$

¹ We consider single-side spectra.

where σ is the Poisson coefficient, Y is the Young modulus of the mirror material, ϕ is the loss angle (we suppose $\phi \ll 1$) and w is the beam waist at the reflecting surface. From Eqs. (1)–(5) we obtain [7,8]

$$S_{\text{Br}}^{\text{single}}(\omega) = \frac{4k_{\text{B}}T}{\pi^{1/2}} \frac{\phi}{\omega} \frac{1}{w} \frac{1 - \sigma^2}{Y}, \quad (6)$$

$$S_{\text{rp}}^{\text{single}} = \left(\frac{2(1 - \sigma^2)F}{\pi^{3/2}cYw} \right)^2 2h\nu P_{\text{in}}. \quad (7)$$

For a FP cavity, the Brownian fluctuations on the two mirrors are independent while the fluctuations due to radiation pressure must be summed coherently obtaining (in the approximation of equal beam size on the mirrors) $S_{\text{Br}}^{\text{FP}} = 2S_{\text{Br}}^{\text{single}}$ and $S_{\text{rp}}^{\text{FP}} = 4S_{\text{rp}}^{\text{single}}$.

For sapphire at 1 K we use the following material parameters: $\phi = 3 \times 10^{-9}$, $\sigma = 0.25$ and $Y = 4 \times 10^{11}$ Pa. With an input laser power of 1 W, a beam waist of 1 mm and a finesse of 10^6 , we get $S_{\text{Br}}^{\text{single}} = 2.7 \times 10^{-44}$ m²/Hz (at 1.3 kHz) and $S_{\text{rp}}^{\text{single}} = 2.9 \times 10^{-42}$ m²/Hz. With such parameters, both effects are larger than the sensitivity limit imposed by the shot-noise. In particular, in order to reduce Brownian noise and radiation pressure fluctuations below this limit we need a beam waist larger than, respectively, 7.4 and 40 mm. If the input power is 7 W, the constraints become as large as 52 and 280 mm.

The optical readout that we have experimented on a room temperature bar is based on a plane-spherical FP cavity with a length of 6 mm and a concave mirror radius of 6 m, giving a spot-size of about 0.18 mm. The plane-spherical geometry does not allow for great improvements, since the cavity length cannot be much increased for obvious technical reasons and for maintaining a low sensitivity to the laser frequency noise, and the dependence of the spot size on the mirror radius R is just as $R^{0.25}$. Other cavity configurations can be used, such as nearly-concentric or meniscus cavities, but the maximum beam-size that can be obtained with reasonable tolerances in the fabrication is few millimeter. An optical geometry alternative to the FP is given by the Herriott delay line [13], where each bounce of the beam corresponds to a different spot. Nakagawa et al. [14] have shown that its thermal noise effect is lower than the one of a FP with the same sensitivity. However, such an optical scheme is only suitable for low corresponding finesse (few hundreds), while the planned finesse of the readout is 10^6 .

In this Letter we present a different optical configuration which allows to keep the sensitivity of a high-finesse FP while using several spots to interrogate two opposite surfaces, as for the Herriott delay line. Our scheme permits to reach the desired low level of thermal noise and radiation pressure effects. The basic idea is to take a long FP cavity and *fold* the optical path, so that the beam experiences several reflections before getting back to the partially reflecting input mirror. This folded Fabry–Perot (FFP) maintains the sensitivity of the high finesse FP (limited by the losses on one single mirror), but the surface fluctuations are probed by several reflections. It is possible to obtain an ‘equivalent’ beam radius of several centimeter maintaining a compact cavity. A similar configuration can be adopted also for the long FP of future generations of long interferometers, by using several mirrors at each end. Such schemes allow to solve completely the problem of excess noise, bringing its effect below the quantum level for the adopted configuration.

2. Design and performance of a folded Fabry–Perot

An example of FFP is shown in Fig. 1(a), where the input mirror is partially reflecting and the others are high reflectors. The input and/or the end mirrors M1 and M4 are concave and the beam experiences several reflections between two intermediate flat mirrors M2 and M3 before reaching M4 and being reflected back. If we call D the distance between the mirrors M2 and M3, θ the incidence angle and N the number of bounces on M2 (there are $N - 1$ bounces on M3) we get an effective cavity length $L = 2ND/\cos\theta$. The geometrical configuration of the beam, i.e., waist dimension, necessary alignment accuracy, etc., is the same as the one of a standard cavity of length L . If the input mirror transmission is T and the losses on each mirror are Σ , we have a

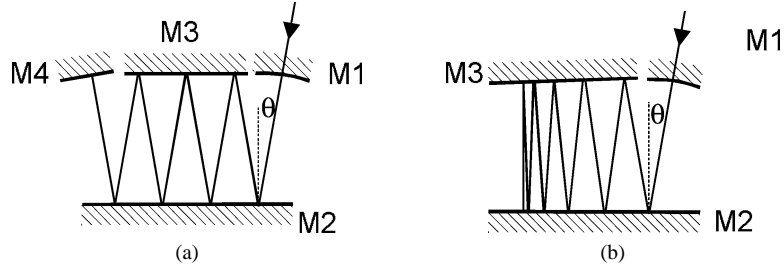


Fig. 1. (a) Folded Fabry–Pérot cavity with input (M1) and end (M4) mirrors, and two parallel intermediate mirrors (M2 and M3): the beam entering the cavity reflects off the intermediate mirrors with a constant incidence angle and bounces back at the end mirrors. (b) Folded Fabry–Pérot cavity with an input mirror (M1) and two angled mirrors (M2 and M3): if the incidence angle of the first reflection on mirror M2 is an integer multiple n of the angle between the mirrors M2 and M3, then the beam bounces back on the same path after $n + 1$ reflections.

total losses coefficient on the round-trip $\Sigma_{\text{TOT}} = 4N\Sigma$. If the Pound–Drever–Hall technique [15] is used to detect the mirror displacement, the optimum signal-to-noise ratio is obtained when $T = \Sigma_{\text{TOT}}$. The cavity finesse is then $F_{\text{FFP}} = 2\pi/(T + \Sigma_{\text{TOT}}) = 2\pi/8N\Sigma$, i.e., a factor of $2N$ lower than the finesse of a simple cavity. The cavity linewidth $\delta_{\text{FFP}} = c/2LF_{\text{FFP}}$ is just a factor of $\cos\theta$ smaller than the one of a Fabry–Pérot cavity of length D made with the same mirrors (M1 and M4).

Simple geometrical considerations show that the shift $\Delta\nu$ of the resonant optical frequency ν due to a change ΔD in the position of M2 is given by $\Delta\nu/\nu = \Delta L/L = \cos^2\theta \Delta D/D$, i.e., for small incidence angles, it is nearly the same as in the case of a simple cavity of length D . A lower limit to the detectable signal is given by the shot noise in the detection and it is proportional to $D\delta_{\text{FFP}}/\nu$. As a consequence, the sensitivity of the FFP is worse by just a factor of $\cos\theta$ with respect to the simple cavity.

We consider now the effect of the Brownian noise. If the thermal fluctuations in the mirror surface position at each spot are not correlated, then the total fluctuations sensed by the beam in a round-trip are given by $S_{\text{Br}}^{2L} = (8N - 2)S_{\text{Br}}^{\text{single}}$, corresponding to relative frequency fluctuations

$$\frac{S_\nu}{\nu^2} = \frac{S_{\text{Br}}^{2L}}{(2L)^2} = \frac{S_{\text{Br}}^{\text{single}} \cos^2\theta}{2D^2} \left(1 - \frac{1}{4N}\right). \quad (8)$$

We have considered that the fluctuations on each spot of M2 and M3 are experienced twice in a round-trip and the two contributions must be summed coherently giving a displacement noise $4(2N - 1)S_{\text{Br}}^{\text{single}}$, while the end mirrors are only sensed ones giving additional contribution $2S_{\text{Br}}^{\text{single}}$.

For a simple cavity of length D the relative frequency noise is $S_\nu/\nu^2 = S_{\text{Br}}^{\text{single}}/2D^2$. This is the first important result: for small incidence angles, the signal remains the same while the excess thermal noise is reduced by about a factor of N (in the power spectrum) with respect to the simple cavity.

In the calculation of the fluctuations in a FFP we must also take into account that the beam size increases with the optical length L . If the concave mirrors radius is much larger than L , we can consider the beam radius w as constant within the FFP and equal to the cavity beam waist w_0 defined below. If we observe the expression in Eq. (6), we see that the displacement power spectrum $S_{\text{Br}}^{\text{single}}$ scales with the inverse of the beam radius. As a consequence, for a rough calculation, we can start from an equivalent radius $w_{\text{E,Br}}$ defined as the beam-size which is necessary to get rid of the Brownian noise in the simple cavity. We find that the minimum number of bounces is given by

$$w_0 = w_{\text{E,Br}} \frac{\cos^2\theta}{N} \left(1 - \frac{1}{4N}\right). \quad (9)$$

If the FFP has one concave mirror with radius R , the beam waist is

$$w_0 = \sqrt{\frac{\lambda z_R}{\pi}} \simeq \left(\frac{2NRD\lambda^2}{\cos\theta\pi^2} \right)^{0.25},$$

where λ is the optical wavelength and $z_R = \sqrt{L(R-L)} \simeq \sqrt{LR}$ is the cofocal parameter. The minimum number of bounces is thus given, for small incidence angles and large N , by

$$N \simeq w_{\text{E,Br}}^{0.8} \left(\frac{\pi}{\lambda} \right)^{0.4} (2RD)^{-0.2}. \quad (10)$$

We analyze now the radiation pressure effect. We must take into account that the radiation pressure scales with the cosine of the incidence angle and that fluctuations on all the spots sums coherently. On the other hand, the intra-cavity power scales with the finesse and it is thus reduced by a factor of $2N$ with respect to the simple cavity. The fluctuations sensed in a round trip are

$$S_{\text{rp}}^{2L} = [(4N-2)\cos\theta + 2]^2 \left(\frac{1}{2N} \right)^2 S_{\text{rp}}^{\text{single}} = 4S_{\text{rp}}^{\text{single}} \cos^2\theta \left(1 + \frac{1-\cos\theta}{2N\cos\theta} \right)^2 \simeq 4S_{\text{rp}}^{\text{single}}. \quad (11)$$

We remark that in the expression of Eq. (7) for $S_{\text{rp}}^{\text{single}}$ the finesse F is the one of a simple cavity, made with the same mirrors of the FFP (M1 and M2). In this way the comparison is simple and the (11) shows that the fluctuations sensed in a round trip of the FFP are nearly the same as the corresponding ones in a simple cavity. The relative frequency noise is

$$\frac{S_v}{v^2} = \frac{S_{\text{rp}}^{2L}}{(2L)^2} = \frac{S_{\text{rp}}^{\text{single}} \cos^4\theta}{4D^2N^2} \left(1 + \frac{1-\cos\theta}{2N\cos\theta} \right)^2 \simeq \frac{S_{\text{rp}}^{\text{single}}}{4D^2N^2}, \quad (12)$$

which is about a factor of $4N^2$ smaller with respect to the relative fluctuations $S_v/v^2 = S_{\text{rp}}^{\text{single}}/D^2$ of a simple cavity.

This is the second important result: while the Brownian noise effect decreases linearly with N , the radiation pressure effect scales even faster, as $1/N^2$.

Like for the Brownian noise, we can define a useful equivalent radius $w_{\text{E,rp}}$ for calculating the necessary number of bounces, which is given by

$$w_0 = w_{\text{E,rp}} \frac{\cos^2\theta}{2N} \left(1 + \frac{1-\cos\theta}{2N\cos\theta} \right). \quad (13)$$

For small incidence angle, we eventually obtain

$$N \simeq \frac{1}{2} w_{\text{E,rp}}^{0.8} \left(\frac{\pi}{\lambda} \right)^{0.4} (RD)^{-0.2}. \quad (14)$$

The expression is similar to the one calculated for the Brownian noise, Eq. (10), but here we must use the larger $w_{\text{E,rp}}$.

3. Numerical estimates and implementation

For a numerical example, we take $R = 10$ m, $D = 6$ mm, $\lambda = 1064$ nm. We have previously quoted the values of 40 and 280 mm for $w_{\text{E,rp}}$, for input power levels of 1 and 7 W. Eq. (14) gives $N = 26$ and $N = 124$ for the two cases. Two consecutive spots on one flat mirror are separated by $d = 2D \tan\theta$. A lower limit to the incidence angle is given by the necessity to limit the scattering losses at the edges of the mirrors. A safe constraint is $d = 4w_0$. With

$N = 26$ we can use $\theta = 0.25$ rad, obtaining an effective cavity length $L = 0.32$ m and a beam waist $w_0 = 0.77$ mm. The flat mirrors width must be $Nd = 80$ mm. For $N = 124$ we have $\theta = 0.35$ rad, $L = 1.6$ m, $w_0 = 1.1$ mm and $Nd = 0.55$ m.

A key point is that the finesse is reduced by a factor of $2N$ with respect to the simple cavity while the beam waist is increased, as we have already remarked. As a consequence, the intra-cavity power is strongly reduced without loosing sensitivity. As an example, for the above considered FFP configurations the light intensity on the mirrors is of the order of 10^4 W/mm². An et al. [16] have already experimented without damage optical cavities with a finesse of 8×10^5 , a waist of $30 \mu\text{m}$ and an input power of 10 mW, giving an intra-cavity intensity as high as 5×10^6 W/mm². The FFP design discussed above can be implemented with the present technology. The spread light absorption also facilitate heat removal.

Different FFP configurations can be adopted, according to the geometry of the masses whose displacement is to be measured. For example, it is possible to avoid the final mirror, thus simplifying the system, by slightly tilting the two flat mirrors, as in Fig. 1(b). If the angle between them is $\theta/2N$, the distance between the spots along the flat mirrors gets shorter and the beam finally gets back on itself. Another interesting design is obtained by increasing the incidence angle and reducing the distance between the parallel mirrors. In the optical transducer implemented for the room-temperature Weber bar [6], a lower limit to the cavity length of about 5 mm is imposed by the tunability range of the Nd:YAG laser. Indeed, it must cover at least one free spectral range if we want to avoid tuning the cavity itself with further complication and possibility to introduce extra-noise sources. On the other hand, in the FFP the distance between resonance peaks is determined by L while the linewidth depends on D . We can thus lower D and reduce the sensitivity to the laser frequency noise. For example, one can chose an angle of 45° , for which high reflectivity coatings have already been tested in ring cavities [17], and reduce D down to about 1 mm.

The design described above is particularly suitable for the proposed dual-cylinder gw detector [4], where the mass displacement has to be measured along a stripe parallel to the cylinder axis. For the dual-sphere gw detector [3] a more compact design can exploit a 2-dimensional configuration, with square flat mirrors where the beam forms a matrix of spots. Several hundreds of spots can be easily obtained with few cm mirrors.

The application of the FFP concept to long baseline interferometers is less obvious, since they already exploit large mirror surfaces to support the wide beam waist. A possible solution is the use of several mirrors, one for each spot. In principle, these mirrors can be hanged on the same suspension, without any extra complication for what concerns the interferometer alignment. A decrease of one order of magnitude in the local fluctuations seems feasible.

4. Calculation including space correlation

The approximated calculation of the Brownian noise for the FFP is based on the assumption that the contributions of the different spots are uncorrelated. On the other hand, Nakagawa et al. [14] give the expressions for the thermal noise of both a standard FP and a delay line, including space correlations, for a half-infinite space. We will now apply their formalism to the FFP, in order to check the validity of the approximated calculation developed above.

We are interested in the noise spectrum for frequencies of few kHz, i.e., well below the cutoff frequency in the response function of the Fabry–Perot which corresponds to the cavity linewidth, i.e., for $\omega < \delta_{\text{FFP}}$. We remind that the linewidth of the FFP is roughly the same as the one of the simple cavity, i.e., tens of kHz. For the sake of simplicity, we will thus omit in the following the response function. We will also use the approximation of small incidence angles ($\cos\theta \simeq 1$).

The effective susceptibility of a mirror with N spots is

$$\chi_N = \chi^{\text{single}} \left\{ N + 2 \sum_{n=2}^N \sum_{q=1}^{n-1} \exp\left(-\frac{|\mathbf{r}_n - \mathbf{r}_q|^2}{2w^2}\right) I_0\left(\frac{|\mathbf{r}_n - \mathbf{r}_q|^2}{2w^2}\right) \right\}, \quad (15)$$

where \mathbf{r}_n is the position of the n th spot, w is the beam radius, assumed as constant, I_0 is the modified Bessel function of the first kind.

The Brownian noise spectrum for a FFP which has N spots on M2 and N' on M3 can be written as

$$S_{\text{Br}}^{\text{FFP}}(\omega) = \frac{4k_{\text{B}}T}{\omega} \phi(4\chi_N + 4\chi_{N'} + 2\chi^{\text{single}}) \quad (16)$$

and inserting the (15) we obtain

$$S_{\text{Br}}^{\text{FFP}}(\omega) = S_{\text{Br}}^{\text{single}}(\omega) \left\{ 4N + 4N' + 2 + 8 \sum_{n=2}^N \sum_{q=1}^{n-1} \exp\left(-\frac{|\mathbf{r}_n - \mathbf{r}_q|^2}{2w^2}\right) I_0\left(\frac{|\mathbf{r}_n - \mathbf{r}_q|^2}{2w^2}\right) + 8 \sum_{n'=2}^{N'} \sum_{q'=1}^{n'-1} \exp\left(-\frac{|\mathbf{r}_{n'} - \mathbf{r}_{q'}|^2}{2w^2}\right) I_0\left(\frac{|\mathbf{r}_{n'} - \mathbf{r}_{q'}|^2}{2w^2}\right) \right\}. \quad (17)$$

For the radiation pressure effect, we can write

$$S_{\text{rp}}^{\text{FFP}} = \left(\frac{2}{c}\right)^2 S_{\text{cav}} |2\chi_N + 2\chi_{N'} + 2\chi^{\text{single}}|^2, \quad (18)$$

and by inserting Eq. (15) and Eq. (3) and using Eq. (7) (where the finesse is the one of the corresponding simple cavity) we obtain

$$S_{\text{rp}}^{\text{FFP}} = S_{\text{rp}}^{\text{single}} \left(\frac{1}{(2N)^2}\right) \left| 4N + 4N' + 2 + 4 \sum_{n=2}^N \sum_{q=1}^{n-1} \exp\left(-\frac{|\mathbf{r}_n - \mathbf{r}_q|^2}{2w^2}\right) I_0\left(\frac{|\mathbf{r}_n - \mathbf{r}_q|^2}{2w^2}\right) + 4 \sum_{n'=2}^{N'} \sum_{q'=1}^{n'-1} \exp\left(-\frac{|\mathbf{r}_{n'} - \mathbf{r}_{q'}|^2}{2w^2}\right) I_0\left(\frac{|\mathbf{r}_{n'} - \mathbf{r}_{q'}|^2}{2w^2}\right) \right|^2. \quad (19)$$

The effect of the interaction between surface fluctuations at different spots can be analyzed directly from the expressions of χ . The right-hand side of Eq. (15) includes a first term,

$$\chi_u = N\chi^{\text{single}},$$

corresponding to uncorrelated noise sources in the different spots, while the remaining terms with double summations accounts for the extra noise due to correlation between spots on the same mirror. The first term gives the noise spectra that we have found in the previous approximated calculations.

In Fig. 2 we report the ratio χ_N/χ_u as a function of the distance d between spots, normalized to the waist, for different configurations of the spots on the mirrors. The excess noise due to correlation rapidly decreases when d gets higher than the beam radius. The approximated calculations described above in this work assumed $d = 4w_0$, and according to the plot in Fig. 2 the susceptibility is correct within a factor of 3 in the case of 1-dimensional array of spots. In this case, the simple expressions derived are an useful tool for a quick estimate of the possible performance and the conceptual validity of the FFP is confirmed by the calculation which includes the correlation terms. This latter contribution becomes more important in the case of 2-dimensional configuration of spots. However, such a design allows for a much higher number of spots in a compact optical system and the desired level of noise can be eventually obtained.

The final result is better express by the relative frequency fluctuations, that can be directly compared with the shot noise. In Fig. 3 we report S_v/v^2 for a FFP with N spots on M2 and $N' = N - 1$ spots on M3, as a function of N , for $P_{\text{in}} = 1$ W and 7 W. The approximated expressions (8) and (12) (with $\cos\theta = 1$) are compared with the results which take into account the correlations between spots, using the complete expressions for the noise densities (17) and (19). The limits corresponding to a simple FP are given by the extrapolation at $N = 0$ of the respective curves.

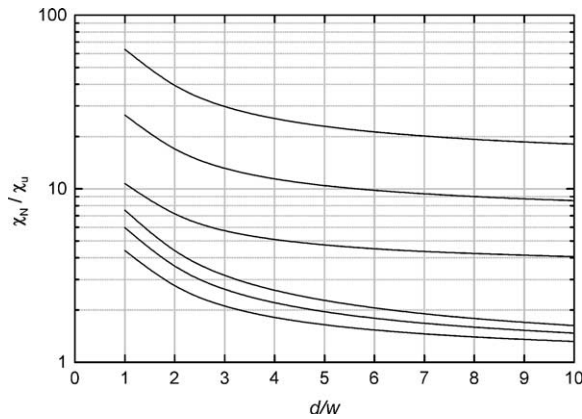


Fig. 2. Ratio between the displacement susceptibility χ_N and its uncorrelated component χ_u as a function of the distance d between spots, normalized to the waist. From lower to higher curves, they correspond to a 1-dimensional linear array, for $N = 25, 100, 400$, and to a 2-dimensional squared array, again for $N = 25, 100, 400$.

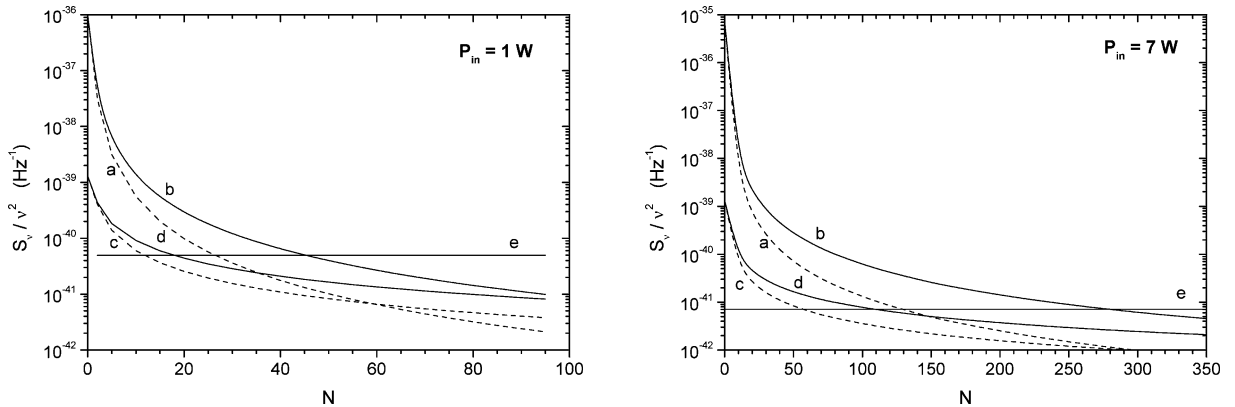


Fig. 3. Relative frequency power noise level S_v/v^2 as a function of the number of spots N on a FFP, for a distance $d = 4w$ between spots and for two different value of impinging power $P_{in} = 1$ W and 7 W. a: Radiation pressure noise without correlation terms; b: radiation pressure noise with correlation terms; c: Brownian noise (at 1300 Hz) without correlation terms; d: Brownian noise (at 1300 Hz) with correlation terms; e: shot noise level. The values at $N = 0$ correspond to the case of a simple FP cavity. The calculation is performed with: $F = 10^6$, $R = 10$ m, $D = 6$ mm and the parameters of sapphire at 1 K.

The shot-noise levels are also reported. The improvement allowed by the FFP is clearly appreciated, as well as the possibility to reach a quantum-limited detection.

5. Conclusion

We have presented an optical cavity configuration which allows to strongly reduce thermal and back-action fluctuations related to the small sensing area of standard cavities.

In this Letter we have used the half-infinite space approximation for calculating the susceptibility. This assumption is valid as soon as the dimension of the surface interrogated is small with respect to the one of the overall detector and, within this limit, our calculation has a general validity and it does not depend on the detector shape.

A more accurate calculation of the detector performance for large interrogation areas cannot distinguish between ‘global’ and ‘local’ effects and one must consider the exact susceptibility of each particular detector and read-out configuration. Calculation methods to accurately evaluate it are presently being developed [18,19]. However, the behavior of the noise reduction predicted in this work allows to closely approach with the present technology the quantum-limited sensitivity calculated for the main mode of the detector, overcoming the problem of the excess noise related to the small beam radius. Such a result is crucial for the design of the next generation of gravitational wave detectors.

Acknowledgements

This work was carried on in the framework of the activity of the group AURIGA of INFN. We thank in particular G. Giusfredi for useful discussions and suggestions, M. Pinard for critical reading of the manuscript and M. Cerdonio for strongly encouraging this work.

References

- [1] LIGO document, M990288-A-M (1999); downloadable as a printable file at the LIGO web site: <http://www.ligo.caltech.edu/docs/M/M990288-A1.pdf>.
- [2] E. Coccia, et al., Phys. Rev. D 57 (1998) 2051.
- [3] M. Cerdonio, et al., Phys. Rev. Lett. 87 (2001) 031101.
- [4] M. Bonaldi, in: Proceedings of GWADW 2002 Workshop, Elba, Italy, 2002; M. Bonaldi, M. Cerdonio, L. Conti, M. Pinard, G.A. Prodi, J.P. Zendri, Phys. Rev. Lett., submitted for publication.
- [5] J.-P. Richard, J. Appl. Phys. 64 (1988) 2202; J.-P. Richard, Phys. Rev. D 46 (1992) 2309.
- [6] M. De Rosa, et al., Class. Quantum Grav. 19 (2002) 1919; L. Conti, et al., gr-qc/0205115, J. Appl. Phys., in press.
- [7] Yu. Levin, Phys. Rev. D 57 (1998) 659.
- [8] Y.T. Liu, K.S. Thorne, Phys. Rev. D 62 (2000) 122002.
- [9] V.B. Braginsky, M.L. Gorodetsky, S.P. Vyatchanin, Phys. Lett. A 264 (1999) 1.
- [10] M. Cerdonio, L. Conti, A. Heidmann, M. Pinard, Phys. Rev. D 63 (2001) 082003.
- [11] A. Heidmann, Y. Hadjar, M. Pinard, Appl. Phys. B 64 (1997) 173.
- [12] L.D. Landau, E.M. Lifshitz, Theory of Elasticity, Pergamon, Oxford, 1986.
- [13] D.R. Herriott, H.J. Schulte, Appl. Opt. 4 (1965) 883.
- [14] N. Nakagawa, E.K. Gustafson, P.T. Beyersdorf, M.M. Fejer, Phys. Rev. D 65 (2002) 082002.
- [15] R.W.P. Drever, J.L. Hall, F. Kowalski, J. Hough, G.M. Ford, A.J. Mulney, H. Ward, Appl. Phys. B 31 (1983) 97.
- [16] K. An, A. Sones, C. Fang-Yen, R.R. Dasari, M.S. Feld, Opt. Lett. 22 (1997) 1433.
- [17] F. Bondu, P. Fritschel, C.N. Man, A. Brillat, Opt. Lett. 21 (1996) 582.
- [18] K. Yamamoto, private communication.
- [19] T. Briant, M. Cerdonio, L. Conti, A. Heidmann, A. Lobo, M. Pinard, Phys. Rev. D, to be submitted.